# An RNA Aptamer Provides a Novel Approach for the Induction of Apoptosis by Targeting the HPV16 E7 Oncoprotein

Clare Nicol, Özlem Cesur, Sophie Forrest, Tamara A. Belyaeva, David H. J. Bunka, G. Eric Blair, Nicola J. Stonehouse*

School of Molecular and Cellular Biology, Faculty of Biological Sciences and Astbury Centre for Structural Molecular Biology, University of Leeds, Leeds, United Kingdom

## Abstract

**Background:** Human papillomavirus 16 (HPV16) is a high-risk DNA tumour virus, which is a major causative agent of cervical cancer. Cellular transformation is associated with deregulated expression of the E6 and E7 oncogenes. E7 has been shown to bind a number of cellular proteins, including the cell cycle control protein pRb. In this study, RNA aptamers (small, single-stranded oligonucleotides selected for high-affinity binding) to HPV16 E7 were employed as molecular tools to further investigate these protein-protein interactions.

**Methodology/Principal Findings:** This study is focused on one aptamer (termed A2). Transfection of this molecule into HPV16-transformed cells resulted in inhibition of cell proliferation (shown using real-time cell electronic sensing and MTT assays) due to the induction of apoptosis (as demonstrated by Annexin V/propidium iodide staining). GST-pull down and bead binding assays were used to demonstrate that the binding of A2 required N-terminal residues of E7 known to be involved in interaction with the cell cycle control protein, pRb. Using a similar approach, A2 was shown to disrupt the interaction between E7 and pRb *in vitro*. Furthermore, transfection of HPV16-transformed cells with A2 appeared to result in the loss of E7 and rise in pRb levels, as observed by immunoblotting.

**Conclusions/Significance:** This paper includes the first characterisation of the effects of an E7 RNA aptamer in a cell line derived from a cervical carcinoma. Transfection of cells with A2 was correlated with the loss of E7 and the induction of apoptosis. Aptamers specific for a number of cellular and viral proteins have been documented previously; one aptamer (Macugen) is approved for clinical use and several others are in clinical trials. In addition to its role as a molecular tool, A2 could have further applications in the future.

**Competing Interests:** The authors have declared that no competing interests exist.

* E-mail: n.j.stonehouse@leeds.ac.uk

## Introduction

Human papillomaviruses (HPVs) are DNA tumour viruses that infect keratinocytes in epithelia. More than 100 types have been identified [1,2] and are classified as either low-risk or high-risk, depending on the associated risk of cancer development. HPV16 is a high-risk virus responsible for approximately 50% of cervical cancers [3,4]. The virus infects cells in the basal layer of cervical epithelia at sites of wounding. Although the majority of infections are cleared by the immune system, persistent infection can lead to development of cancer. Cellular transformation is initiated through deregulated expression of the viral oncogenes E6 and E7 [5,6]. High-risk E6 has been shown to promote degradation of the tumour suppressor p53 [7,8], while E7 binds and destabilises the cell cycle control protein pRb [9,10]. E7 binds the hypophosphorylated form of pRb, inhibiting its interaction with E2F transcription factors, leading to deregulated progression to the S-phase of the cell cycle [11]. In addition to this well characterised

role, E7 has been shown to interact with more than 30 other cellular proteins including p300 and TATA binding protein (TBP) [12,13]. We have recently reported the selection of RNA aptamers to HPV16 E7 for use as novel molecular tools [14]. Aptamers are short nucleic acids that fold into complex three dimensional structures and bind target molecules in a conformation-dependent manner. Aptamers have potential to rival antibodies in many applications due to their high binding affinity and ability to discriminate between closely related targets. Furthermore, they can be very small (therefore reaching targets that may be inaccessible to antibodies). Nucleic acid aptamers are single-stranded oligonucleotides whereas peptide aptamers are composed of a variable peptide loop attached to a protein scaffold. The former have the advantage in that they are able to undergo multiple rounds of denaturation and re-folding. In addition, they are non-immunogenic and can be synthesised to very high purity and modified in a number of ways to increase their stability, for example by inclusion of modified nucleotides [15,16,17]. They can

be produced *in vitro* to virtually any target by a process known as Systematic Evolution of Ligands by Exponential Enrichment (SELEX) [18,19,20] and delivered to live cells by lipofection. In some cases, certain aptamers have also been shown to be internalised by receptor-mediated endocytosis. This opens up many avenues for development of novel therapeutics as well as tools for the investigation of protein function [21,22]. Unlike siRNAs which act at the level of mRNA to affect protein expression, nucleic acid aptamers act directly on protein molecules, thus allowing finer control. Such aptamers have been generated to a variety of viral proteins including the HCV protease NS3 [23] and polymerase NS5B [24], SARS coronavirus helicase [25], H5N1 influenza HA [26], FMDV 3D polymerase [27] and several HIV proteins including gp120, reverse transcriptase and the trans-activator protein Tat [21].

Our E7 RNA aptamers [14] were stabilised against nucleases and spontaneous degradation by the inclusion of 2′-fluoro modified pyrimidines [28,29]. After selection, we sequenced 20 individual clones and found some that grouped into families based on sequence similarity. Several representative clones were screened for binding to GST-E7. As one of the highest affinity binders, aptamer A2 was selected for further study. The sequence and predicted secondary structures of A2 (lowest energy structures) are shown in Figure S1. Here, we show that this molecule inhibits cellular proliferation via induction of apoptosis in an HPV16-transformed cervical carcinoma cell line (SiHa) that actively expresses both E6 and E7 [30], but not in the control cell lines, HaCaT (a keratinocyte cell line) [31] and C33A (a cervical carcinoma cell line derived from an HPV-negative cancer) [32] or the HPV18 cell line, HeLa [33]. We also demonstrate that this aptamer binds to the region of E7 required for interaction with pRb and is capable of blocking the interaction of E7 with cellular pRb *in vitro*. Furthermore, transfection of the HPV16-positive cervical cancer cell line, CaSki [30], with this aptamer appeared to result in a loss of the E7 oncoprotein and in a rise in cellular pRb levels.

## Results

### Inhibition of Cellular Proliferation and Induction of Apoptosis in HPV16-Postitive Cells with Aptamer A2

We have previously reported the selection of RNA aptamers against the oncogenic HPV16 protein E7 and demonstrated that aptamer A2 binds to GST-E7 *in vitro* [14]. In order to assess A2-mediated effects on cells expressing E7, cell growth rates were analysed. SiHa cells were selected for this study as these cells constitutively express both E6 and E7. The cells are derived from a human cervical carcinoma and have 1 or 2 copies of the HPV16 genome integrated into chromosome 13 [30]. HaCaT (immortalised keratinocyte) cells were used as a negative control. Cells were transfected with up to 100 nM A2 and analysed after 24 or 48 hours by MTT assay. No significant changes in cell viability were measured after 24 hours, (Figure 1A), however, SiHa cells transfected with A2 had reduced cell viability after 48 hours, compared to mock-transfected cells (a reduction of between $22.9\pm3.0$ and $34.4\pm0.9\%$). No alteration in growth was detected in HaCaT cells (Figure 1B).

The observations above were confirmed with the use of a real-time cell electronic sensing (RT-CES) system (xCELLigence, Roche), which measures cellular proliferation via the electrical impedance conferred on a microelectrode array [34,35]. In brief, cells were allowed to adhere to microelectrode-coated 96-well plates for 18 hours prior to transfection with either A2 or an aptamer selected to an unrelated protein (the RNA-dependent-RNA polymerase of FMDV) as a negative control (referred to as SF1). This aptamer contains the same primer sequences as A2 and

only differs in the $N_{30}$ random region, thus sharing 61.5% similarity. The predicted lowest energy structures of both A2 and SF1 are shown in Figure S1. It should be noted that 2′F modifications can affect the pucker of the ribose which is not taken into account in this folding algorithm. Therefore, the predicted structures are an approximation and may not accurately represent aptamer structure in solution. Cellular proliferation rates were measured in triplicate as change in electrical impedance (cell index) over time (Figures 1C to F). Transfection was performed in serum-free media for 4 hours and corresponded with a rapid drop in impedance (arrowed, i). However, this returned to approximately the pre-transfection level, in most cases, upon addition of serum (arrowed, ii). Both SiHa and HaCaT cells mock-transfected with lipofection reagent alone continued to proliferate over time. However, the proliferation rate fell rapidly when cells were treated with staurosporine as an inducer of apoptosis [36,37]. The subsequent small rise in cell index observed with SiHa cells is consistent with some cells surviving staurosporine treatment. Transfection of SiHa cells with aptamer A2 caused the cell index to decrease over time (Figure 1C). The effect was rapid in cells transfected with 100 nM A2, in which the decrease in cell index commenced at 8 hours post-transfection. After 24 hours the cell index had fallen by $32.6\pm4.4\%$. With reduced concentration of A2 there was delayed onset of effect; the cell index of SiHa cells transfected with 50 or 25 nM A2 did not begin to decrease until 18 and 22 hours post-transfection, respectively. This did not reach the levels seen with 100 nM A2. After 48 hours post-transfection, there was a dose-dependent decrease in cell index of $59.0\pm1.9\%$, $63.1\pm3.3\%$ and $75.6\pm1.5\%$ with 25, 50 and 100 nM A2, respectively. The slight increase in the cell index recorded immediately after recovery with serum is likely to reflect changes in cell morphology and adhesion consistent with the induction of apoptosis. Other studies using this system for the analysis of cytotoxic compounds have observed similar cell index profiles [38,39,40]. In contrast, HaCaT cells (which do not express E7) were unaffected at any concentration of A2 tested (Figure 1D). Furthermore, the negative control aptamer, SF1, had no significant effect on the proliferation of either SiHa or HaCaT cells (Figures 1E and F respectively).

The changes in cell index measured by RT-CES were greater than the changes in viability measured by MTT assay. This could reflect insensitivity of the latter, or that the real-time cell sensing assay may over-estimate reductions in cell growth because of changes in cell morphology. The appearance of SiHa cells after transfection with A2 was indicative of induction of apoptosis, whilst HaCaT cells appeared unaffected (Figure 2A). To quantify this observation, apoptosis assays were performed in which SiHa cells were transfected with increasing concentrations of aptamer (up to 200 nM). After 24 hours, samples were stained with FITC-conjugated annexin V and propidium iodide to identify apoptotic cells by flow cytometry. A small increase in apoptosis was induced in SiHa cells transfected with the control aptamer SF1, $9.25\pm1.9\%$ and $11.2\pm2.0\%$ at 100 nM and 200 nM, respectively (Figure 2B). However, the level of apoptosis in cells transfected with A2 was greater, with $18.0\pm3.4\%$ and $23.7\pm1.7\%$ apoptosis at 100 nM and 200 nM A2, respectively (Figure 2B). For both concentrations of A2 used, the level of total apoptosis increased in a dose-responsive manner and was significantly higher than that induced by SF1 ($p<0.05$ and $p<0.01$, respectively). This was due to an increase in both early and late apoptosis 24 hours after transfection with A2. The level of A2-induced apoptosis therefore accounts for a large proportion of the observed decrease in growth (33%) of SiHa cells at 24 hours post-transfection with 100 nM A2, shown
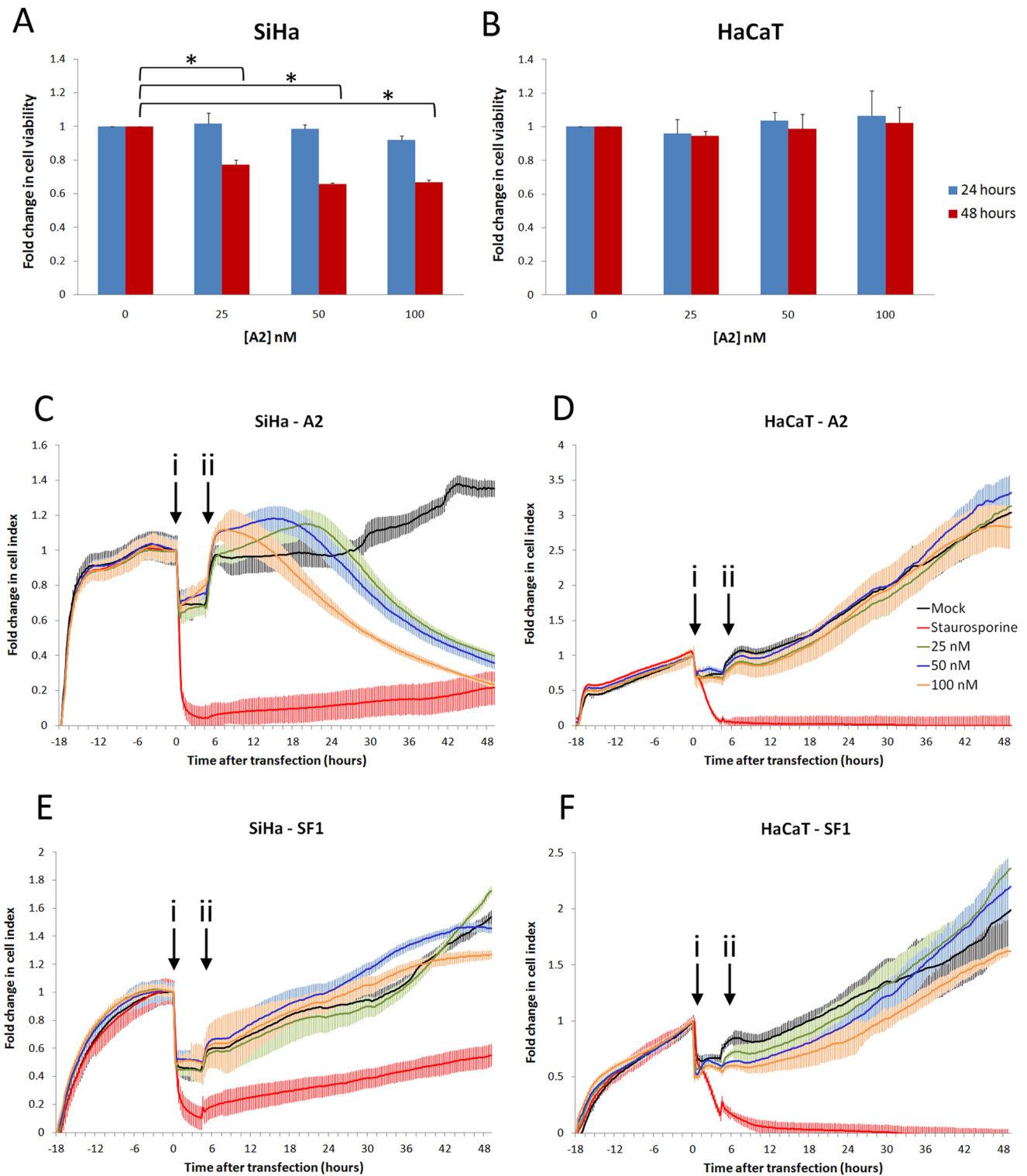
**Figure 1. Reduction of cell growth in HPV16-transformed cells by aptamer A2.** A2 was transfected into SiHa (A) or HaCaT (B) cells at concentrations of 0, 25, 50 or 100 nM. Cells were incubated for 24 or 48 hours and metabolically active cells were identified by MTT assay. Data are presented as fold change in cell growth compared with mock-treated cells. Standard errors of three separate experiments are shown. *indicates $p < 0.05$. SiHa (C and E) or HaCaT (D and F) cells were seeded at 10,000 per well of a Roche E-plate and allowed to adhere for 18–21 hours. Cells were then transfected with 25, 50 or 100 nM of either A2 (panels C and D) or control aptamer SF1 (panels E and F) and incubated in serum-free media for 4 hours. Serum was added to a final concentration of 10% (v/v) and cells analysed by the Roche xCELLigence system for a further 48 hours. The average of 3 experiments and standard errors are shown. i = transfection with aptamer; ii = addition of serum.
doi:10.1371/journal.pone.0064781.g001

in Figure 1C. Although there was a small increase in apoptosis seen in HaCaT cells, there was no significant difference in the levels induced by A2 or SF1 (Figure 2C), in contrast to that observed in SiHa cells. It should be noted that although HaCaT is an HPV-negative cell line, it is not derived from a cervical carcinoma. We therefore extended studies to include two additional cervical carcinoma cell lines: HeLa cells (HPV18-positive) and C33A cells (HPV-negative). Figures 2D and 2E demonstrate that both SF1 and A2 have a small effect on the level of apoptosis measured in both HeLa and C33A cells, however, neither of these increases was significantly different and are likely to have resulted from a non-specific response to the presence of the RNA. The data also indicates that there is HPV-type specificity of A2, appearing to having little effect on HPV18 E7-expressing cells, however further experiments would be necessary to confirm this. It should be noted that the innate immune response in HeLa cells has been shown to be much reduced compared to C33A cells [41]. Therefore, if the results seen here were due exclusively to innate immunity, we would have expected to see a greater effect in C33A than in HeLa cells. We would also have expected to see similar effects of SF1 and A2 in SiHa cells. In contrast, these data collectively suggest that the effect of A2 on SiHa cell proliferation is at least in part due to an induction of targeted apoptosis. As similar effects were seen in HaCaT, C33A and HeLa cells, HaCaT cells were used as a control cell line for further experiments.

## A2 Binds at the N-terminus of HPV16 E7

E7 has three conserved regions and has been shown to bind pRb via a LXCXE motif in conserved region 2 (CR2) (Figure 3A) [42,43,44]. In contrast, binding of E7 to p300 involves residue 2 in CR1 as well as residue 24 in the LXCXE motif [45] and the binding of TBP requires residues in the zinc-binding domain of CR3 [46]. To identify regions of the E7 protein involved in the interaction with A2, a panel of mutant GST-E7 proteins [45] was expressed in *E. coli*, purified (Figure 3B) and binding assays performed, as previously reported [14,27,47]. In brief, purified proteins were bound to glutathione-magnetic (GM) beads and incubated with $[\gamma^{32}P]$-labelled A2. The percentage of bound aptamer was determined by scintillation counting of the bound and unbound fractions. Although maximal binding was not achieved in these experiments, by comparing the data in a qualitative manner it can be seen that binding of A2 to E7 was moderately affected by small deletions in the zinc-binding domain ($\Delta 2$ or $\Delta 4$), however, binding was abrogated by point mutations at residues 2 or within the LXCXE motif at position 24 (Figure 3C), indicating that A2 binds at the N-terminus of E7. Furthermore, the changes seen in A2-E7 binding as a result of point mutations/deletions in E7, provides support for the interaction between E7 and A2 being specific, rather than E7 acting as a general RNA-binding protein.

## Disruption of the Interaction between E7 and pRb by Aptamer A2 *in vitro*

As both aptamer A2 and the pRb protein require residues in the N-terminal region of E7 for binding, we predicted that our aptamer might disrupt interactions between E7 and pRb. Indeed, our previous preliminary studies demonstrated that A2 had the ability to interfere with interactions between pRb and GST-E7 [14]. We therefore carried out further GST pull-down assays to quantify this effect (Figures 4A and B). For these experiments we used HaCaT cell lysate, as these cells do not express E7 and would therefore provide a source of pRb in the absence of endogenous E7 that could interfere with the binding assay. HaCaT lysate (lane 1) was incubated with GST-E7 (54 µM) immobilised onto GM-beads. In the absence of A2 (lane 2), pRb was precipitated by

GST-E7, however, with increasing concentrations of A2 (lanes 3–5) the amount of pRb precipitated by GST-E7 was reduced. GST alone did not interact with pRb in either the absence or presence of A2 (lanes 6 and 7, respectively). These data confirm that A2 is able to disrupt the E7-pRb interaction *in vitro* in a dose-dependent manner, by up to 96% at the highest concentration tested (15 µg, 11 µM) (Figure 4B).

To further investigate the effect of A2 on the E7-pRb interaction, we performed co-immunoprecipitation assays in the presence or absence of aptamer. For this analysis, 100 nM A2 or SF1 was transfected into CaSki cells, a cervical cancer cell line containing several hundred copies of the HPV16 genome [30]. These cells express E7 at approximately a 6-fold higher level than SiHa cells (O. Watherston, pers. comm.). Of note, the high level of E7 expression in CaSki cells meant that it was not possible to deliver sufficient aptamer in order to detect statistically significant levels of apoptosis (Figure S2). However, the E7 level was sufficient for detection by immunoblotting and thus allowed the effect of aptamer to be determined. After transfection, cells were incubated for 24 hours, followed by preparation of cell lysates and immunoprecipitation with antibodies to E7 or pRb. The experiment therefore allows quantification of levels of E7 and pRb in two ways; by co-immunoprecipitation and by comparison of input levels after 24 hours incubation with aptamer. In both mock-transfected and SF1-transfected samples, efficient co-immunoprecipitation of E7 was observed using anti-pRb (Figure 5A, lanes 4 and 6, respectively). However, when 100 nM A2 was transfected into the cells, co-immunoprecipitation of E7 by anti-pRb was reduced by 80% (comparing lanes 4 and 5). This is mirrored by the reduction of the input level of E7 in cells transfected with A2 for 24 hours (Figure 5A, lanes 1–3). A2 transfection reduced the level of E7 in these cells by 75% (comparing lanes 1 and 2), whilst in cells which received the SF1 control, the level of E7 was reduced by only 18% (comparing lanes 1 and 3). The A2-mediated reduction in E7 levels correlated with an increase in cellular pRb, as the total level of pRb in cells which had been transfected with 100 nM A2 for 24 hours was increased 5-fold (comparing the pRb doublet in lanes 7 and 8). However, when the cell lysate was immunoprecipitated with anti-E7, there was no difference in the level of co-immunoprecipitation of pRb by anti-E7 in any of the treatments (lanes 10–12). This was possibly due to the high level of E7 expression in these cells, coupled with the concentration of E7 by antibody binding. To investigate this further, the level of E7 in CaSki cells in the presence or absence of aptamer was investigated. CaSki cells were transfected with aptamer, incubated for 24 hours and E7 levels then detected by immunoblot. Figure 5B shows that in cells that were either mock-transfected (lane 1) or transfected with the control aptamer SF1 (lane 3) the level of E7 was significantly higher than in cells transfected with A2 (lane 2). Densitometry analysis of 4 independent experiments (Figure 5C) showed that in CaSki cells transfected with A2, the level of E7 was reduced by $62.7\pm10.5\%$ (lane 2), while in SF1-transfected cells the level was reduced by only $15.0\pm15.7\%$ (lane 3). Together, these results indicate that during the 24 hour incubation with A2, E7 had been lost from the cells. Experiments were also performed to investigate the effects of A2 on levels of endogenous pRb. As a result of A2 transfection, pRb levels were elevated. Although there was a degree of variability in the level detected, on average, almost three-fold increase over mock transfection was measured ($271.9\pm112.1\%$), as shown in Figures 5D and E, comparing lanes 1 and 2. Transfection with the control aptamer SF1 (lane 3) had little effect ($116.2\pm26.5\%$).
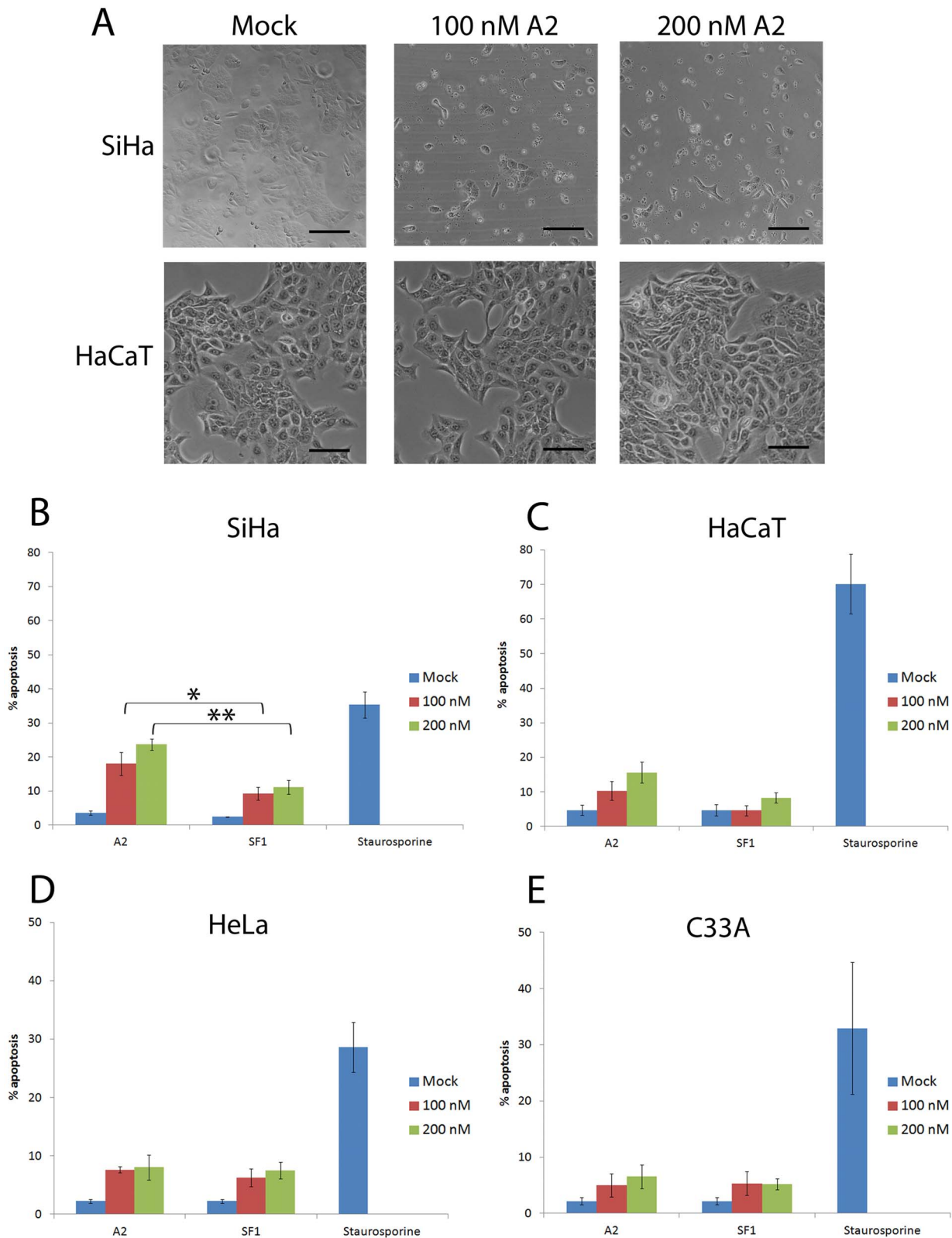
**Figure 2. Cell death on transfection with aptamer A2.** (A) SiHa or HaCaT cells were either mock transfected or transfected with 100 nM or 200 nM A2 and maintained for 48 hours. Shown are bright-field microscopy images. Scale bar: 100 μm. (B) SiHa, (C) HaCaT, (D) HeLa and (E) C33A cells were either mock-transfected, treated with staurosporine at 0.5 μM or transfected with either A2 or control aptamer SF1 to final concentration of 100 or 200 nM and analysed for apoptosis after 24 hours. Cells were dual-stained with FITC-conjugated annexin V and propidium iodide. Graphs show total % apoptosis and standard errors of at least three separate experiments. *indicates p<0.05, **indicates p<0.01.
doi:10.1371/journal.pone.0064781.g002
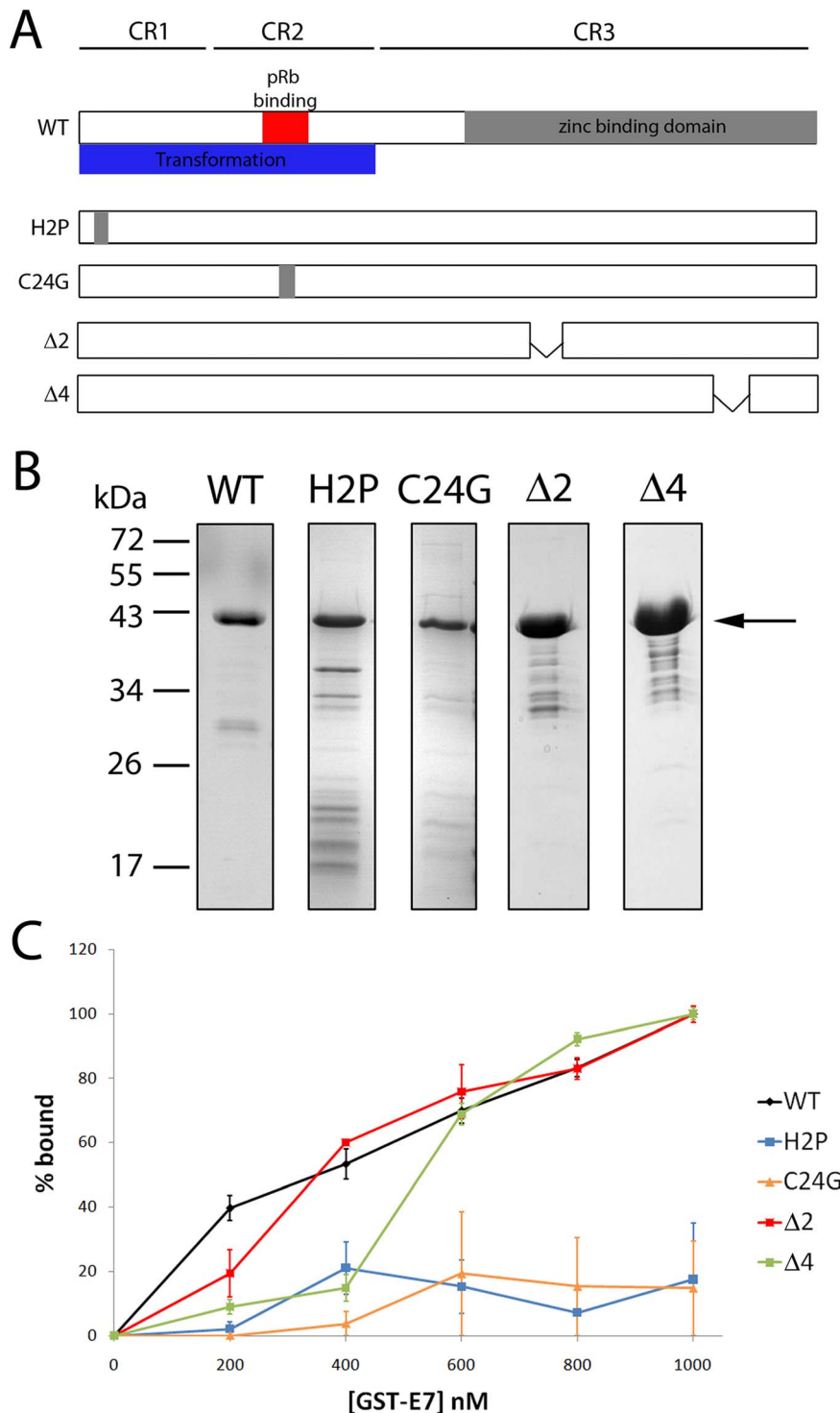
**Figure 3. Binding of aptamer A2 to wild-type and mutant HPV16 E7 proteins.** (A) Schematic representation of the HPV16 E7 protein indicating point mutations and deletions. (B) SDS-PAGE analysis of E7 proteins after expression, purification and binding to GM-beads. Samples were visualised by Coomassie staining. Arrow indicates full-length protein. (C) A2 was 5′ end-labelled with [γ$^{32}$P]-ATP and incubated with increasing concentrations of bead-bound protein. GST-only beads were included to maintain a constant volume of beads. % bound RNA was quantified by scintillation counting. A2 was probed for binding to wild-type (WT) GST-E7, GST-E7-Δ2, GST-E7-Δ4, GST-E7 H2P and GST-E7 C24G. Data shown is the average of 3 replicates and standard error.
doi:10.1371/journal.pone.0064781.g003
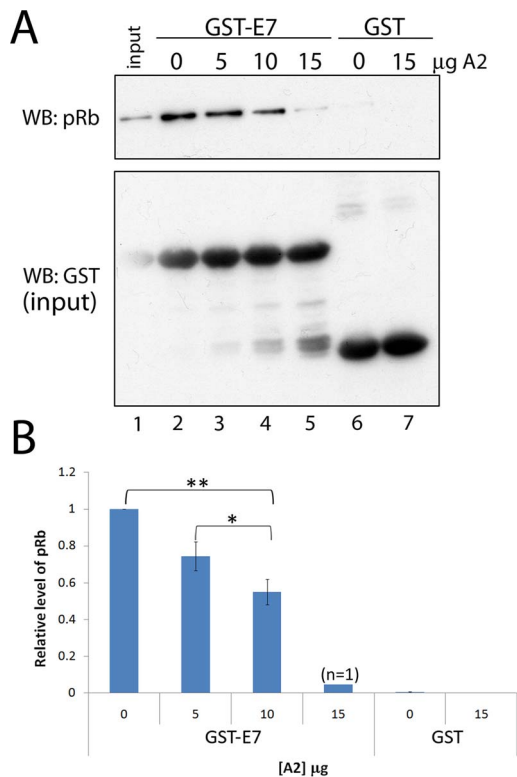
**Figure 4. Disruption of the interaction between HPV16 E7 and pRb by aptamer A2 *in vitro*.** (A) GST pull-down assay in the presence and absence of aptamer A2. 1 µg of GST-E7 (54 µM) bound to GM-beads was incubated with 300 µg of protein from a HaCaT cell lysate (as a source of pRb) for 1 hour at 4°C in the presence of 0, 5, 10 or 15 µg of A2. Bead-bound GST alone was incubated with either 0 or 15 µg (11 µM) A2. GST proteins and interacting proteins were isolated from the reaction and analysed by immunoblot using antibodies to pRb and GST. (B) Densitometric analysis of the interaction between GST-E7 and pRb in the absence and presence of A2, standard errors relating to three separate experiments are shown. *indicates p<0.05, **indicates p<0.01.
doi:10.1371/journal.pone.0064781.g004

## Discussion

RNA aptamers are currently employed as tools to investigate a variety of viral and cellular proteins [21] and also for development in diagnostics and as anti-viral agents [48,49]. We have characterised an RNA aptamer (termed A2) selected against the HPV16 oncoprotein E7. Transfection of A2 into an HPV16-transformed cell line (SiHa) resulted in decreased cell viability by the induction of apoptosis. This aptamer was able to inhibit the interaction between HPV16 E7 and pRb *in vitro*. Upon further investigation, it appeared that transfection of CaSki cells with this molecule resulted in a reduction in E7 levels and that this loss appeared to correlate with an increase in the levels of pRb. However, it is not known whether A2 can affect the levels of other related pocket proteins such as p300.

Both pro- and anti-apoptotic effects of E7 have been reported in the literature. Our data are consistent with an anti-apoptotic effect of E7 in SiHa and CaSki cells. E7 is extremely unstable in the cell and is rapidly ubiquitinated and degraded via the proteasome [50,51]. E7 proteins from high-risk HPVs have a high degree of intrinsic protein disorder (especially at the pRb-binding N-terminus) which is greater than that displayed by E7 proteins from low-risk types [52,53,54]. This flexibility may contribute to

its ability to bind to a variety of proteins. It is possible that A2-mediated inhibition of the critical E7-pRb interaction could result in E7 instability and degradation, thus allowing restoration of pRb levels. Although it appears from the results reported here that A2 can result in disruption of the E7-pRb interaction *in vitro*, it is unclear if this also can occur in the context of the cell. It is therefore possible that A2 binding directly induces the loss of E7, resulting in a restoration of pRb levels. A previous study has shown that expression of constitutively-active pRb in cervical cancer cell lines resulted in the induction of apoptosis [55]. We suggest that the loss of E7 that was detected upon transfection of A2 resulted in a release of active pRb, ultimately resulting in an apoptotic response. It remains possible that the slight increases in apoptosis seen with the control aptamer SF1 are due to the presence of modified nucleotides or innate RNA sensing. However, these effects are small in comparison with the effects of A2 and therefore the main mode of action of A2 is unlikely to be a result of the innate immune response to aptamer RNA.

Interestingly, a similar result to that reported here has been observed with the use of an E7 siRNA. Although E7 protein levels were not measured directly, an increase in hypophosphorylated pRb was demonstrated which correlated with induction of apoptosis [56]. However, we (and others) have also observed different effects of E7 siRNAs e.g. growth arrest [57]. It should be noted that the mode of action of siRNA molecules is to interfere with protein synthesis at the translational level. As E6 and E7 are expressed from a single bicistronic mRNA, the use of siRNA can result in the down-regulation of both proteins and in off-target effects, possibly explaining the different results documented [58]. Although off-target effects remain a possibility here, we have demonstrated little effect of A2 in three HPV16-negative cell lines (HeLa, C33A and HaCaT). Using pull-down assays, we have also demonstrated that A2 had no effect on the interaction between p53 and E6 (data not shown/Belyaeva et al, in preparation).

Our data are also supported by several reports of the pro-apoptotic effects of E7-targeted peptides [59,60,61]. Furthermore, one of these molecules was demonstrated to act via reactivation of the pRb/E2F pathway, consistent with the effects of the RNA aptamer A2, described here. Although peptide aptamers can be costly to produce at high purity, together these studies demonstrate the power of these approaches in the development of potential novel therapeutics. Recently, a separate study has identified further RNA aptamers to HPV16 E7 [62]. Although these were not characterised in cells, this work further illustrates the potential of this technology. The use of E7 aptamers as specific molecular tools is therefore likely to be helpful in dissecting these pathways and in understanding the complex roles of E7.

Our previous studies have demonstrated that small sequence variations in A2 have affected the ability of the aptamer to affect the E7-pRb interaction [14]. Further characterisation of A2 may identify a minimal binding region and thus allow generation of a smaller molecule, cheaper and easier to produce. Work is ongoing to characterise other E7 aptamers from the selected pool [14] and aptamers to HPV16 E6, as targeting both oncoproteins is likely to have an additive effect. Studies are also on-going to further investigate the pathway of E7 loss, the specificity of the aptamers and aptamer delivery into primary cells. Aptamer technology thus has the potential to provide new insights into the multiple molecular interactions performed by these small viral oncoproteins.
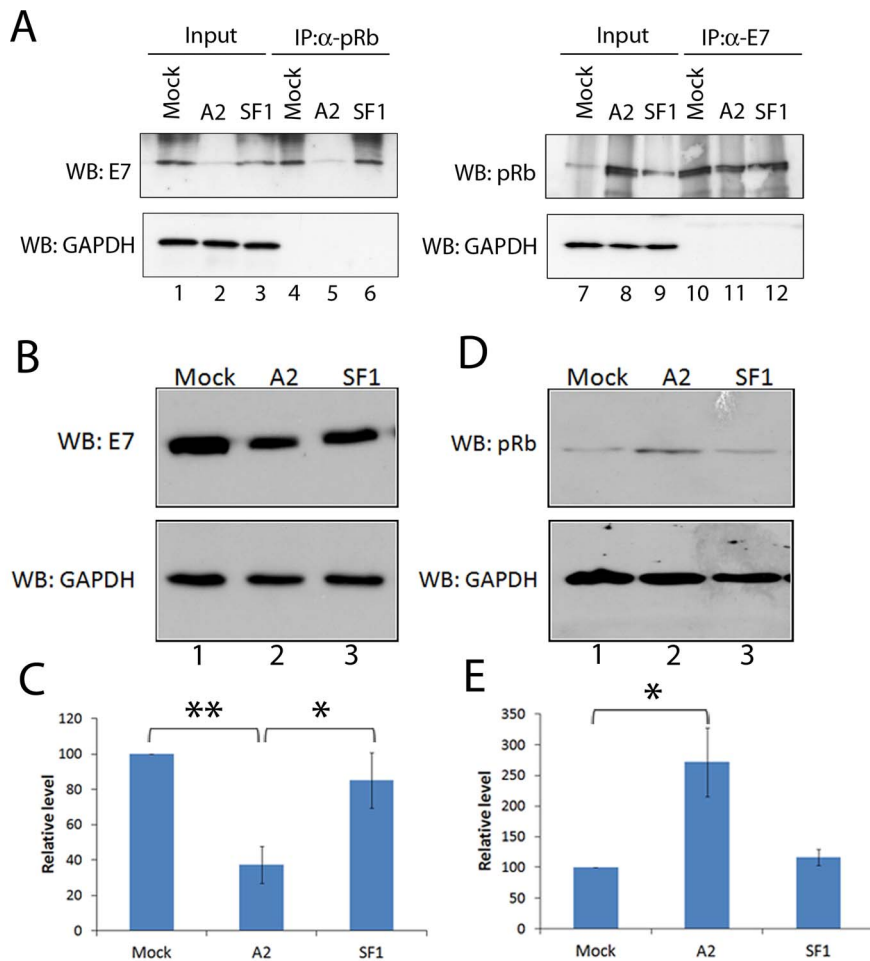
**Figure 5. Reduction of HPV16 E7 protein levels in CaSki cells following transfection of aptamer A2.** (A) Co-immunoprecipitation of pRb and HPV16 E7 in the presence or absence of aptamer. CaSki cells were either mock-transfected or transfected with A2 or SF1 at a final concentration of 100 nM and incubated for a further 24 hours before lysis and co-immunoprecipitation with 2 μg of either anti-pRb or anti-E7. Immunoblot analysis was performed for the detection of E7, pRb or GAPDH. Values of densitometric analysis and lane numbers are included below the gels for reference in the text. (B) CaSki cells were mock-transfected or transfected with either 100 nM A2 or SF1 (control aptamer) and incubated for 24 hours. Cells were lysed in Laemmli buffer. Immunoblot analysis was then performed to detect E7 and GAPDH. Lane numbers are included below the gels for reference in the text. (C) Graph shows the results and standard errors of 4 separate experiments, with E7 levels shown as % mock. *indicates $p < 0.05$, **$p < 0.01$. (D) CaSki cells were mock-transfected or transfected with either 100 nM A2 or SF1 (control aptamer) and incubated for 24 hours. Cells were lysed in Laemmli buffer. Immunoblot analysis was then performed to detect pRb and GAPDH. Lane numbers are included below the gels for reference in the text. (E) Graph shows the results and standard errors of 4 separate experiments, with pRb levels shown as % mock. *indicates $p < 0.05$.
doi:10.1371/journal.pone.0064781.g005

## Materials and Methods

### Protein Expression and Purification

Expression and purification of GST-E7 was undertaken following our previous published protocols [14]. Expression vectors for E7 with point mutations or deletions were also described previously [46,63].

### Cell Culture and Antibodies

SiHa [64], CaSki [65], HeLa (HPV-positive human cervical cancer-derived) [66], C33A (HPV-negative human cervical cancer-derived) [67] and HaCaT (immortalised keratinocyte) [31] cells were maintained in DMEM supplemented with 10% (v/v) FCS, 100 units/ml penicillin, 0.1 mg/ml streptomycin and 1% (w/v) glutamine at 37°C and 5% (v/v) $CO_2$. Antibodies used were anti-pRb (4H1, New England Biolabs and 1F8, AbCam), anti-16E7 (NM2, Santa Cruz), anti-GST (P1A12, Cambridge

Bioscience), rabbit anti-pRb (Ab-2, Merck Chemicals) and anti-GAPDH (Sigma Aldrich).

### Aptamer Synthesis

*In vitro* selections were performed using the Biomek 2000 Automated Workstation (Beckman Coulter) as described previously [14]. *In vitro* transcription reactions were carried out including 2′-fluoro-UTP and 2′-fluoro-CTP (TriLink Biotechnologies), using a mutant T7 RNA polymerase [68], according to the method reported previously [14]. A2 and SF1 share 5′ and 3′ regions i.e. GGGAAUGGAUCCACAUCUACGAAU–$N_{30}$–UU-CACUGCAGACUUGACGAAGCUU. Sequences of the $N_{30}$ regions were CCCUUCAUCAUUAACCCGUCCACGCGC and UCGGCUCAAAAAUACGUCCGCACCAUACA for A2 and SF1, respectively.

## Cell Proliferation Assays

a) Measurement of cell viability was undertaken using the MTT assay. Cells were seeded at $10^4$ per well of a 96-well plate and incubated for 24 hours prior to transfection with increasing concentrations of aptamer (0, 25, 50 and 100 nM). Cells were maintained for a further 48 hours at $37°C$, followed by incubation with 20 µl of 5 mg/ml 3-(4,5-Dimethylthiazol-2-yl)-2,5-diphenyltetrazolium bromide (MTT) in PBS for 4 hours at $37°C$. Formazan crystals were dissolved by incubation with acidic isopropanol (96% isopropanol/4% 1M HCl) for one hour at $37°C$. Absorbance was measured at $\lambda = 570$ nm with background subtraction at 630 nm.

b) Real-time monitoring of cellular proliferation was performed using the xCELLigence system (Roche, UK). Cells were seeded at $10^4$ per well of a micro-electrode coated 96-well plate and allowed to adhere for 17–21 hours. Cells were either mock-transfected or transfected with aptamer using Oligofectamine (Invitrogen) and maintained at $37°C$ with monitoring every 15 minutes. Automatic analysis by the RTCA software generated a measurement of cell proliferation based on the electrical impedance conferred on the micro-electrodes by the presence of cells (termed cell index).

## Apoptosis Assays

Cells ($1.5 \times 10^5$) were seeded into 4 cm$^2$ wells 24 hours prior to transfection with up to 200 nM of A2 or SF1 as described above and maintained at $37°C$ for 24 hours. Cells were harvested by trypsinisation, washed twice with PBS and suspended in ice cold annexin V buffer (10 mM HEPES-KOH (pH 7.4), 140 mM NaCl and 2.5 mM CaCl$_2$) with FITC-conjugated annexin V and incubated on ice for 15 minutes. Cells were co-stained with propidium iodide at 50 µg/ml in PBS and analysed using the FACSCalibur and Cellquest Pro software (Becton Dickinson).

## Aptamer Binding Assays

Radiolabelled aptamer RNA was generated by 5′ end-labelling with [$\gamma^{32}$P]-ATP, unincorporated nucleotides were removed by column purification (NucAway spin column, Ambion). Labelled RNA was incubated with protein-loaded GM-beads at a final concentration of 1 nM for 30 minutes at room temperature. Protein-loaded beads and any bound RNA were isolated from the reaction mixture and the supernatant transferred to scintillation fluid (unbound fraction). Beads were washed three times with PBS and suspended into scintillation fluid (bound fraction). The method is based on our previously reported protocols [14,27,47].

## GST Pull-down Assays

GST and GST-E7 proteins were bound to GM-beads and cell lysates prepared as described previously [14]. After incubation for 1 hour at $4°C$, beads were isolated, washed and samples analysed by immunoblotting using anti-GST and mouse anti-pRb.

## Co-immunoprecipitation Assays

Cells ($3 \times 10^5$) in 6-well plates were transfected with 100 nM aptamer using Oligofectamine. Cells were lysed in RIPA buffer and cleared by centrifugation. Lysate was incubated with 2 µg of anti-E7 or anti-pRb overnight at $4°C$ with shaking. Antibody-lysate mixtures were centrifuged to remove precipitates followed by incubation with 20 µl of a 50% (v/v) protein G sepharose slurry (Sigma) for 2 hours. Sepharose was collected by centrifugation and washed with RIPA buffer three times before re-suspension in SDS-PAGE loading buffer and analysis by immunoblotting.

## Statistical Analysis

Standard errors are included, and a student's T-test was performed to obtain p-values, where appropriate.

## Supporting Information

**Figure S1 Structure predictions for aptamers A2 and SF1 as calculated by Mfold [69].** Three structures were predicted for A2, with 2 for SF1. ΔG values, as calculated by Mfold, are given.
(TIF)

**Figure S2 Apoptotic response of CaSki cells to aptamer.** CaSki cells were either mock-transfected, treated with staurosporine at 0.5 µM or transfected with either A2 or control aptamer (DB) to final concentration of 200 nM and analysed for apoptosis after 24 hours. Cells were dual-stained with FITC-conjugated annexin V and propidium iodide. Graphs show total % apoptosis. Standard error bars are shown were appropriate.
(TIF)

## Acknowledgments

## Author Contributions

Conceived and designed the experiments: NS GEB. Performed the experiments: CN ÖC TB DB. Analyzed the data: CN NS. Contributed reagents/materials/analysis tools: SF GEB DB NS. Wrote the paper: CN GEB NS.

## References

1. de Villiers E-M, Fauquet C, Broker TR, Bernard H-U, zur Hausen H (2004) Classification of papillomaviruses. Virology 324: 17–27.
2. Bernard H-U, Burk RD, Chen Z, van Doorslaer K, zur Hausen H, et al. (2010) Classification of papillomaviruses (PVs) based on 189 PV types and proposal of taxonomic amendments. Virology 401: 70–79.
3. Muñoz N, Bosch FX, Castellsagué X, Díaz M, de Sanjose S, et al. (2004) Against which human papillomavirus types shall we vaccinate and screen? The international perspective. International Journal of Cancer 111: 278–285.
4. Parkin DM, Bray F (2006) Chapter 2: The burden of HPV-related cancers. Vaccine 24: S11–S25.
5. Jeon S, Lambert PF (1995) Integration of human papillomavirus type 16 DNA into the human genome leads to increased stability of E6 and E7 mRNAs: implications for cervical carcinogenesis. Proceedings of the National Academy of Sciences (USA) 92: 1654–1658.
6. Pett M, Coleman N (2007) Integration of high-risk human papillomavirus: a key event in cervical carcinogenesis? Journal of Pathology 212: 356–367.
7. Scheffner M, Werness BA, Huibregtse JM, Levine AJ, Howley PM (1990) The E6 oncoprotein encoded by human papillomavirus types 16 and 18 promotes the degradation of p53. Cell 63: 1129–1136.
8. Lechner MS, Laimins LA (1994) Inhibition of p53 DNA binding by human papillomavirus E6 proteins. Journal of Virology 68: 4262–4273.
9. Dyson N, Howley PM, Munger K, Harlow E (1989) The human papilloma virus-16 E7-oncoprotein is able to bind to the retinoblastoma gene-product. Science 243: 934–937.
10. Boyer SN, Wazer DE, Band V (1996) E7 protein of human papilloma virus-16 induces degradation of retinoblastoma protein through the ubiquitin-proteasome pathway. Cancer Research 56: 4620–4624.

11. Chellappan S, Kraus VB, Kroger B, Munger K, Howley PM, et al. (1992) Adenovirus E1A, simian virus 40 tumor antigen, and human papillomavirus E7 protein share the capacity to disrupt the interaction between transcription factor E2F and the retinoblastoma gene product. Proceedings of the National Academy of Sciences (USA) 89: 4549–4553.

12. zur Hausen H (2000) Papillomaviruses causing cancer: evasion from host-cell control in early events in carcinogenesis. Journal of the National Cancer Institute 92: 690–698.

13. Wise-Draper T, Wells S (2008) Papillomavirus E6 and E7 proteins and their cellular targets. Frontiers in Bioscience 13: 1003–1017.

14. Nicol C, Bunka DHJ, Blair GE, Stonehouse NJ (2011) Effects of single nucleotide changes on the binding and activity of RNA aptamers to human papillomavirus 16 E7 oncoprotein. Biochemical and Biophysical Research Communications 405: 417–421.

15. Blank M, Blind M (2005) Aptamers as tools for target validation. Current Opinion in Chemical Biology 9: 336–342.

16. Bunka DH, Stockley PG (2006) Aptamers come of age - at last. Nature Reviews Microbiology 4: 588–596.

17. Mayer G (2009) The Chemical Biology of Aptamers. Angewandte Chemie International Edition 48: 2672–2689.

18. Ellington AD, Szostak JW (1990) In vitro selection of RNA molecules that bind specific ligands. Nature 346: 818–822.

19. Robertson DL, Joyce GF (1990) Selection in vitro of an RNA enzyme that specifically cleaves single-stranded DNA. Nature 344: 467–468.

20. Tuerk C, Gold L (1990) Systematic evolution of ligands by exponential enrichment: RNA ligands to bacteriophage T4 DNA polymerase. Science 249: 505–510.

21. James W (2007) Aptamers in the virologists' toolkit. Journal of General Virology 88: 351–364.

22. Ni X, Castanares M, Mukherjee A, Lupold SE (2011) Nucleic acid aptamers: clinical applications and promising new horizons. Current Medicinal Chemistry 18: 4206–4214.

23. Fukuda K, Umehara T, Sekiya S, Kunio K, Hasegawa T, et al. (2004) An RNA ligand inhibits hepatitis C virus NS3 protease and helicase activities. Biochemical and Biophysical Research Communications 325: 670–675.

24. Biroccio A, Hamm J, Incitti I, De Francesco R, Tomei L (2002) Selection of RNA aptamers that are specific and high-affinity ligands of the hepatitis C virus RNA-dependent RNA polymerase. Journal of Virology 76: 3688–3696.

25. Jang KJ, Lee N-R, Yeo W-S, Jeong Y-J, Kim D-E (2008) Isolation of inhibitory RNA aptamers against severe acute respiratory syndrome (SARS) coronavirus NTPase/Helicase. Biochemical and Biophysical Research Communications 366: 738–744.

26. Cheng C, Dong J, Yao L, Chen A, Jia R, et al. (2008) Potent inhibition of human influenza H5N1 virus by oligonucleotides derived by SELEX. Biochemical and Biophysical Research Communications 366: 670–674.

27. Ellingham M, Bunka DHJ, Rowlands DJ, Stonehouse NJ (2006) Selection and characterization of RNA aptamers to the RNA-dependent RNA polymerase from foot-and-mouth disease virus. RNA 12: 1970–1979.

28. Beigelman L, McSwiggen JA, Draper KG, Gonzalez C, Jensen K, et al. (1995) Chemical modification of hammerhead ribozymes. Journal of Biological Chemistry 270: 25702–25708.

29. Pieken WA, Olsen DB, Benseler F, Aurup H, Eckstein F (1991) Kinetic characterization of ribonuclease-resistant 2'-modified hammerhead ribozymes. Science 253: 314–317.

30. Baker CC, Phelps WC, Lindgren V, Braun MJ, Gonda MA, et al. (1987) Structural and transcriptional analysis of human papillomavirus type 16 sequences in cervical carcinoma cell lines. Journal of Virology 61: 962–971.

31. Boukamp P, Petrussevska RT, Breitkreutz D, Hornung J, Markham A, et al. (1988) Normal keratinization in a spontaneously immortalized aneuploid human keratinocyte cell line. Journal of Cell Biology 106: 761–771.

32. Yee C, Krishnan-Hewlett I, Baker C, Schlegel R, Howley P (1985) Presence and expression of human papillomavirus sequences in human cervical carcinoma cell lines. American Journal of Pathology 119: 361–366.

33. Mincheva A, Gissmann L, zur Hausen H (1987) Chromosomal integration sites of human papillomavirus DNA in three cervical cancer cell lines mapped by in situ hybridization. Medical Microbiology and Immunology 176: 245–256.

34. Boyd JM, Huang L, Xie L, Moe B, Gabos S, et al. (2008) A cell-microelectronic sensing technique for profiling cytotoxicity of chemicals. Analytica Chimica Acta 615: 80–87.

35. Kirstein SL, Atienza JM, Xi B, Zhu J, Yu N, et al. (2006) Live cell quality control and utility of real-time cell electronic sensing for assay development. Assay and Drug Development Technologies 4: 545–553.

36. Couldwell WT, Hinton DR, He S, Chen TC, Sebat I, et al. (1994) Protein kinase C inhibitors induce apoptosis in human malignant glioma cell lines. FEBS Letters 345: 43–46.

37. Rüegg U, Burgess G (1989) Staurosporine, K-252 and UCN-01: potent but nonspecific inhibitors of protein kinases. Trends in Pharmacological Sciences 10: 218–220.

38. Abassi YA, Xi B, Zhang W, Ye P, Kirstein SL, et al. (2009) Kinetic cell-based morphological screening: prediction of mechanism of compound action and off-target effects. Chemistry and Biology 16: 712–723.

39. Xing JZ, Zhu L, Gabos S, Xie L (2006) Microelectronic cell sensor assay for detection of cytotoxicity and prediction of acute toxicity. Toxicology in Vitro 20: 995–1004.

40. He X, Wang J, Steele J, Sun X, Nie W, et al. (2009) An ultrasensitive rapid immunocytotoxicity assay for detecting Clostridium difficile toxins. Journal of Microbiological Methods 78: 97–100.

41. Yu S-L, Chan P, Wong C-K, Szeto C-C, Ho S, et al. (2012) Antagonist-mediated down-regulation of toll-like receptors increases the prevalence of human papillomavirus infection in systemic lupus erythematosus. Arthritis Research & Therapy 14: R80.

42. Barbosa MS, Edmonds C, Fisher C, Schiller JT, Lowy DR, et al. (1990) The region of the HPV E7 oncoprotein homologous to adenovirus E1A and SV40 large T antigen contains separate domains for Rb binding and casein kinase II phosphorylation. EMBO Journal 9: 153–160.

43. Jones RE, Wegrzyn RJ, Patrick DR, Balishin NL, Vuocolo GA, et al. (1990) Identification of HPV-16 E7 peptides that are potent antagonists of E7 binding to the retinoblastoma suppressor protein. Journal of Biological Chemistry 265: 12782–12785.

44. Liu X, Clements A, Zhao K, Marmorstein R (2006) Structure of the human papillomavirus E7 oncoprotein and its mechanism for inactivation of the retinoblastoma tumor suppressor. Journal of Biological Chemistry 281: 578–586.

45. Bernat A, Avvakumov N, Mymryk JS, Banks L (2003) Interaction between the HPV E7 oncoprotein and the transcriptional coactivator p300. Oncogene 22: 7871–7881.

46. Massimi P, Pim D, Banks L (1997) Human papillomavirus type 16 E7 binds to the conserved carboxy-terminal region of the TATA box binding protein and this contributes to E7 transforming activity. Journal of General Virology 78: 2607–2613.

47. Robinson MA, Wood JPA, Capaldi SA, Baron AJ, Gell C, et al. (2006) Affinity of molecular interactions in the bacteriophage phi29 DNA packaging motor. Nucleic Acids Research 34: 2698–2709.

48. Gopinath SCB (2007) Antiviral aptamers. Archives of Virology 152: 2137–2157.

49. Bunka DHJ, Platonova O, Stockley PG (2010) Development of aptamer therapeutics. Current Opinion in Pharmacology 10: 557–562.

50. Oh K-J, Kalinina A, Wang J, Nakayama K, Nakayama KI, et al. (2004) The papillomavirus E7 oncoprotein is ubiquitinated by UbcH7 and Cullin 1- and Skp2-containing E3 ligase. Journal of Virology 78: 5338–5346.

51. Reinstein E, Scheffner M, Oren M, Ciechanover A, Schwartz A (2000) Degradation of the E7 human papillomavirus oncoprotein by the ubiquitin-proteasome system: targeting via ubiquitination of the N-terminal residue. Oncogene 19: 5944–5950.

52. Garcia-Alai MM, Alonso LG, de Prat-Gay G (2007) The N-terminal module of HPV16 E7 is an intrinsically disordered domain that confers conformational and recognition plasticity to the oncoprotein. Biochemistry 46: 10405–10412.

53. Ohlenschlager O, Seiboth T, Zengerling H, Briese L, Marchanka A, et al. (2006) Solution structure of the partially folded high-risk human papilloma virus 45 oncoprotein E7. Oncogene 25: 5953–5959.

54. Uversky VN, Roman A, Oldfield CJ, Dunker AK (2006) Protein intrinsic disorder and human papillomaviruses: increased amount of disorder in E6 and E7 oncoproteins from high risk HPVs. Journal of Proteome Research 5: 1829–1842.

55. Ryan JB, Wesley AB, Susanne IW, Erik SK (2009) Activation of the retinoblastoma tumor suppressor mediates cell cycle inhibition and cell death in specific cervical cancer cell lines. Molecular Carcinogenesis 48: 45–55.

56. Jiang M, Milner J (2002) Selective silencing of viral gene expression in HPV-positive human cervical carcinoma cells treated with siRNA, a primer of RNA interference. Oncogene 21: 6041–6048.

57. Bottley G, Watherston OG, Hiew YL, Norrild B, Cook GP, et al. (2007) High-risk human papillomavirus E7 expression reduces cell-surface MHC class I molecules and increases susceptibility to natural killer cells. Oncogene 27: 1794–1799.

58. Yamato K, Yamada T, Kizaki M, Ui-Tei K, Natori Y, et al. (2007) New highly potent and specific E6 and E7 siRNAs for treatment of HPV16 positive cervical cancer. Cancer Gene Therapy 15: 140–153.

59. Guo C, Liu K, Luo H, Chen H, Zheng Y, et al. (2011) Potent anti-tumor effect generated by a novel human papillomavirus (HPV) antagonist peptide reactivating the pRb/E2F pathway. PLoS ONE 6: e17734.

60. Guo C, Liu K, Zheng Y, Luo H, Chen H, et al. (2011) Apoptosis induced by an antagonist peptide against HPV16 E7 in vitro and in vivo via restoration of p53. Apoptosis 16: 606–618.

61. Nauenburg S, Zwerschke W, Jansen-Dürr P (2001) Induction of apoptosis in cervical carcinoma cells by peptide aptamers that bind to the HPV-16 E7 oncoprotein. FASEB Journal 15: 592–594.

62. Toscano-Garibay JD, Benítez-Hess ML, Alvarez-Salas LM (2011) Isolation and characterization of an RNA aptamer for the HPV-16 E7 oncoprotein. Archives of Medical Research 42: 88–96.

63. Edmonds C, Vousden KH (1989) A point mutational analysis of human papillomavirus type 16 E7 protein. Journal of Virology 63: 2650–2656.

64. Friedl F, Kimura I, Osato T, Ito Y (1970) Studies on a new human cell line (SiHa) derived from carcinoma of uterus. I. Its establishment and morphology. Proceedings of the Society for Experimental Biology and Medicine 135: 543–545.

65. Pattillo R, Hussa R, Story M, Ruckert A, Shalaby M, et al. (1977) Tumor antigen and human chorionic gonadotropin in CaSki cells: a new epidermoid cervical cancer cell line. Science 196: 1456–1458.

66. Gey GO, Coffman WD, Kubicek MT (1952) Tissue culture studies of the proliferative capacity of cervical carcinoma and normal epithelium. Cancer Research 12: 264–265.

67. Auersperg N (1964) Long-term cultivation of hypodiploid human tumor cells. Journal of the National Cancer Institute 32: 135–163.

68. Padilla R, Sousa R (2002) A Y639F/H784A T7 RNA polymerase double mutant displays superior properties for synthesizing RNAs with non-canonical NTPs. Nucleic Acids Research 30: e138.

69. Zuker M (2003) Mfold web server for nucleic acid folding and hybridization prediction. Nucleic Acids Research 31: 3406–3415.